Current Research in Environmental Sustainability 3 (2021) 100052

Contents lists available at ScienceDirect

Current Research in Environmental Sustainability

journal homepage: www.sciencedirect.com/journal/current-research-in-environmental-sustainability

Integrating support vector machine and cellular automata for modelling land cover change in the tropical rainforest under equatorial climate in Ghana

Clement Nyamekye [a,*], Samuel Kwofie [b], Emmanuel Agyapong [a], Samuel Anim Ofosu [a], Richard Arthur [c], Linda Boamah Appiah [d]

[a] Department of Civil Engineering, Koforidua Technical University, P. O. Box KF981, Koforidua, Ghana
[b] Department of Applied Statistics, Koforidua Technical, University, Koforidua, Ghana
[c] Department of Energy Systems Engineering, Koforidua Technical University, P. O. Box KF981, Ghana
[d] Department of Environmental Management and Technology, Koforidua Technical University, P. O. Box KF981, Koforidua, Ghana

ARTICLE INFO

Keywords:
Support vector machine
Tropical rainforest
CA-Markov
Land use change

ABSTRACT

Unsustainable anthropogenic activities such as indiscriminate logging of trees, mineral exploitation, conversion of forest into agricultural lands are known to cause major environmental changes, thereby triggering a chain of irreversible forest depletion. This has called an urgent need by government and private agencies to institute policies and programs to curtail the destruction of the ecosystem due to the pressure on the available land. In this study, the Land use/land cover changes between the period of 1986 and 2020 in the tropical rainforest of Ghana was considered. A combination of machine learning and Markov chain approach was adopted to project future LULC for 2040 and 2060.The results showed that area covered by Open Forest declined from 21,531.87 km^2 to 14,518.82 km^2 and Dense Forest also declined from 14,313 km^2 to 8202.98 km^2 over a period of 34 years. The CA-Markov model was used to predict the future land use land cover, and it was observed that the total forest cover could decline to 15,551.79 km^2 in 2040 and further decrease to 13,401.79 km^2 in 2060. It was also found that settlement, mining and agricultural land, which is be driven by rapid population increase, has contributed significantly to the rapid declining forest cover. The results of this study have demonstrated the impact of unsustainable use of natural resources in these three regions. It also highlights the need for concerted effort to develop comprehensive environmental policies to encapsulate sustainable conversion and utilisation of natural resources by focusing on water-energy-food nexus.

1. Introduction

The impacts of land use land cover changes (LULCC) on the sustainability of ecologies have become an increasingly significant subject in environmental discourse on the global scale (Acheampong et al., 2018).

Current trends of LULC in sub-Saharan Africa (SSA) depict an increasing unsustainable slue in the conversion of natural vegetation into different land use forms (Kutiote et al., 2019; Näschen et al., 2019). Both natural and human-induced land cover variations have been observed to influence global changes in land use, and subsequent effect on climate change(Haque and Basak, 2017). Furthermore, the interactions of human with the ecosystem and biodiversity have led to ecological sustainability issues (Islam et al., 2018; Trisurat et al., 2019). For example, the rapid increase population has immensely increased the demand for natural resources such as land, water, energy, food etc., resulting in depletion of the forest for agriculture and removal of plants for purposes such as illegal mining and urbanization. Thus, population growth, socio-economic development and urbanization exert significant pressure on the scarce natural resources of a country, which contributes significantly to changes in land cover especially forests (Asabere et al., 2020; Simms, 2008; Yang et al., 2020) whiles threatening the biodiversity. Such anthropogenic activities have long-term direct bearing on climate change.

In view of the relevance of forest resources in Ghana and its necessity for sustainable development, the country has joined the International

* Corresponding author.
E-mail address: nyamekyeclement@gmail.com (C. Nyamekye).

https://doi.org/10.1016/j.crsust.2021.100052
Received 11 April 2021; Received in revised form 20 May 2021; Accepted 22 May 2021
Available online 27 May 2021

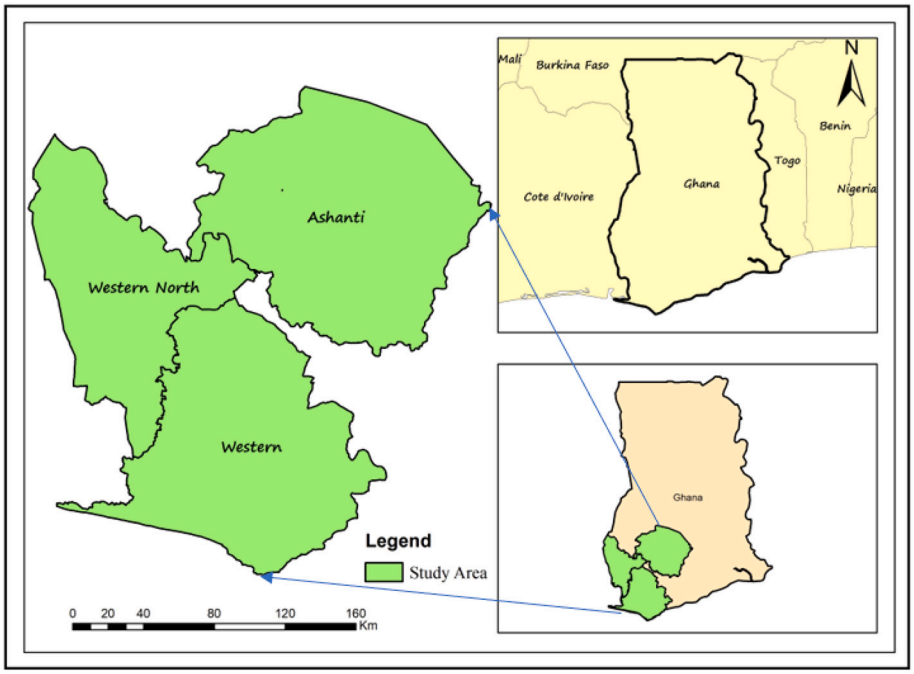

Fig. 1. Map of the three regions making up the study area.

Action on Reducing Emissions, Deforestations and Forest Degradation (REDD) (Oduro et al., 2015; Satyal, 2018). The purpose for joining is to safeguard the biodiversity and habitats, while conserving the basis of livelihoods for the growing population. This is in line with the UN Agenda 2030 and African Union Agenda 2063 that were espoused in 2015 at the UN general assembly and Assembly of Heads of States and Government of the AU in Addis Ababa respectively. The Sustainable Development Goals (SDGs) focus mainly on actions to pursue economic development, while ensuring social and environmental sustainability on the basis of good governance. Nevertheless, the ability to institute concrete national strategies and frameworks to address sustainability issues, while pursuing economic development and prosperity is absent due to insufficient scientific evidence and data to inform and assist decision making. Thus, it is imperative to comprehend the underlying process of change to better derive targeted policies and frameworks to support efficient planning of land use, management and restoration of the ecology that conforms to the requirements of the SDGs, towards climate change adaptation and mitigation. Information on current LULC should provide essential information that could be used to support decision making process, while the modelled prediction about credible future LULC scenarios should also provide indications for potential trends and a basis for identifying solutions. Current improved and available satellite data coupled with complex technologies has enabled researches to project LULC change in the future (e.g., Ahmed and Ahmed, 2012; Beaumont and Duursma, 2012). Additionally, modelling LULC change is becoming much critical (Herold et al., 2002), as time will be used to report projected changes at different temporal and spatial scales. Some examples of common models that have been used for predicting and simulating future LULC changes include, Markov Chain Analysis (MCA) or Markov Model (Hamad et al., 2018; Sivakumar, 2014), Cellular Automata (Sinha et al., 2015); Binary Logistic Regression (Zeng et al., 2019), and Cellular -Automata-Markov Model (CA-Markov) (Subedi et al., 2013).

Also, declining forest cover continuously remains to be a matter of critical concern for natural resources and environmental managers, policy makers and governmental agencies. This therefore, calls for adequate research into forest cover dynamics in Ghana by delving into changes in the land use/land cover across forest zones. However, there is insufficient information on changes LULC and it is therefore imperative to address this research gap for the proper management of the forest cover in the study. Hence, this study aimed at assessment, quantification and prediction of the future LULC changes in the tropical rainforest in Ghana. This was guided by a change analysis of classified Landsat imagery to assess and quantify the past changes, the development of land change model, using a combination of machine learning and Markov chain approach to project future LULC for 20,400 and 2060.

2. Materials and method

2.1. Study area

The study was conducted in three regions in Ghana, namely, Ashanti, Western and Western North region, all situated in the southern part, constituting the tropical rainfall forest of Ghana. The Ashanti region with its administrative capital Kumasi, is located between longitudes $0^{o}15' - 2^{o}$ 25′W and latitudes $5^{o}50'$-$7^{o}40'$N and has a total land mass of 24, 389 km^2. The region also experiences double rainfall regimes in a year, with maximum in May/June and minimum in October. The average annual rainfall ranges between 1100 mm and 1800 mm and mean annual temperature ranging between 25.5 °C and 32 °C. The region is characterised by two types of vegetation; the northern part is described as the Guinea Savanna (short deciduous and fire-resistant trees), whiles the southern part is characterised with the semi-deciduous forest. It has about 22.5% of Ghana's forest reserve, which makes it the second largest producer of cocoa in Ghana. The Western North region was originally part of the Western region before the reorganisation of the regions in 2018. The Western and Western North regions share a common boundary and are also bounded to the West by Ivory Coast, Central region to east and the southeast, respectively. The Western and Western North regions have Sekondi-Takoradi and Wiawso

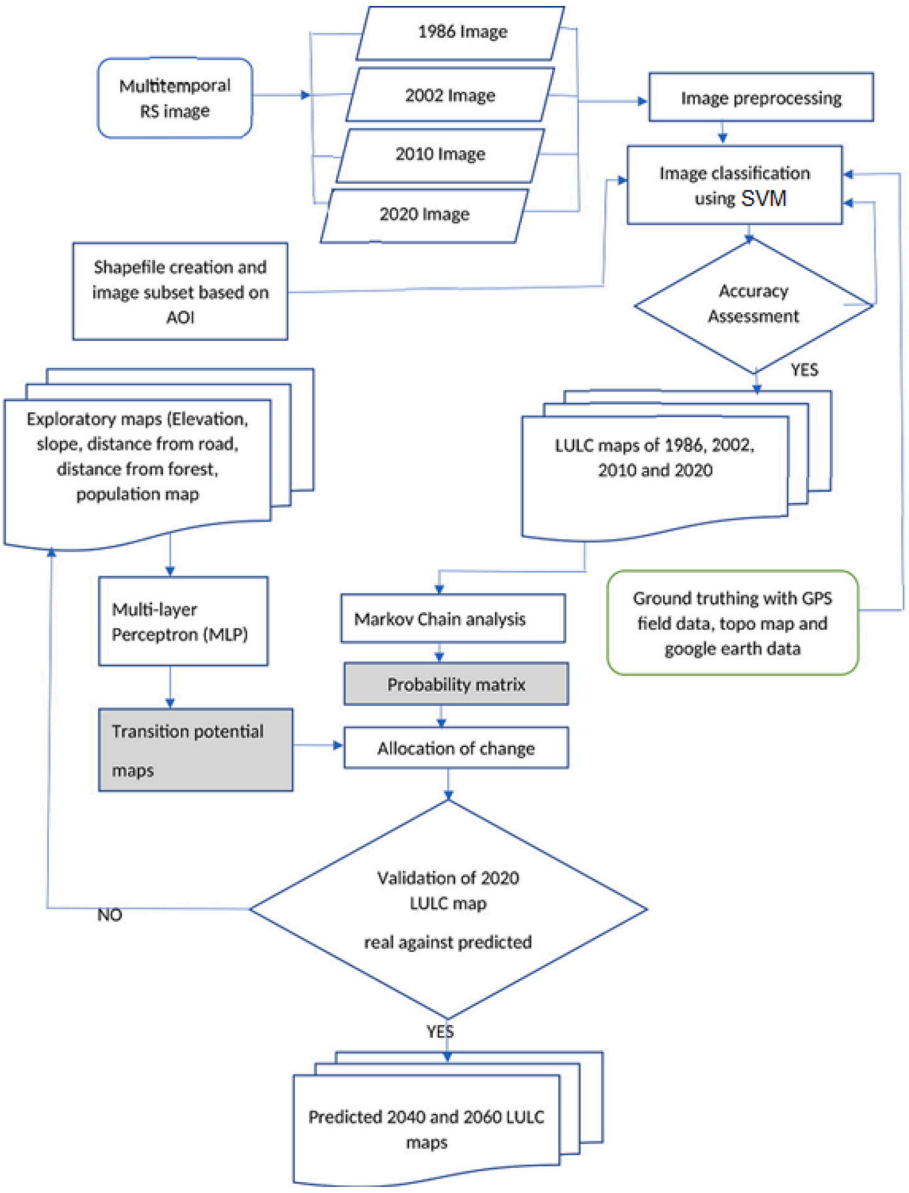

Fig. 2. Flow chart of the overall method.

as their capital and both covering a total land area of 23, 921 km^2. The two regions are described as the wettest part of the country with two rainfall regimes, i.e., the major one between April to July and the minor one between September and October (Lossou et al., 2019). The average annual rainfall in these two regions range between 12,500 mm to 2000 mm and mean annual temperature range between 26 °C to 30 °C. These regions lie in the equatorial climatic zone with 75% of the vegetation within the forest zone of Ghana, making it the largest producer of cocoa in the country. All the three regions in this study are endowed with significant natural resources such as gold, bauxite, iron, diamond and manganese, which makes mining a predominant activity in the area. (Fig. 1).

2.2. Data collection

Landsat TM images of 1986, 2002, 2010 and OLI image of 2020, which all covered the tropical rainforest of Ghana were used for this research. It also included administrative and topographical map, ASTER GDEM, road and population map. The remote sensing images were originally obtained from the United States Geological Survey (USGS) archive (https://earthexplorer.usgs.gov). The images were geometrically corrected and the spatial coordinate system was WGS 84 to UTM Zone 32 N. The administrative and topographic map, as well as the road maps were obtained from the Municipal assemblies. The population data used in generating the map was obtained from the Ghana statistical service (GSS). The selection of the images was based on the following principles (i) The period when the vegetation cover could be detected since forest and agricultural land covers are eminent in this study; (2) Only with less than 15% cloud cover were used in the stacking process, which resulted in about 70–80% useable tile for each of the four-year period considered. Based on these principles, all the images were acquired from November to March. From the dataset, five criteria, including: slope, altitude, distance from road map, distance from forest edges and population map were chosen for additional analysis. The

input data were the four LULC maps, and the exploratory data being slope, distance from road and population map.

2.3. Methodology

The method adopted in this study to produce the LULC maps and to also predict the future LULC maps was developed using different tools and theoretical framework (Fig. 2).

2.3.1. Training of model and pre-processing

Before training the model, pre-processing was performed in R environment. The pre-processing of satellite images is important for the analysis (Dagnachew et al., 2020). Activities such as atmospheric correction, normalization, layer stacking, image registration, geometric correction, image enhancement and cloud masking were carried out during the pre-processing stage (Abd El-Kawy et al., 2011; Kogo et al., 2019; Langat et al., 2019; Muriithi, 2016). Furthermore, the normalization process scaled the predictors values between 0 and 1, so as to make sure that no one feature dominate the others. This is essential for efficient execution of the machine learning models, especially Support Vector Machine (SVM) and deep learning classifiers (Liu et al., 2017).

2.3.2. Classification model development

The processing of the satellite image and the classification of the LULC maps was carried out using SVM, which is a well-known Machine Learning (ML) algorithms for supervised classification and post-classification analysis within the R programming environment (Devlelopment Core Team, 2013). SVM uses Kernel functions and structural risk minimization theory (Vapnik, 2013). This algorithm has been widely applied in many remote sensing researches (Mountrakis et al., 2011) and the model used the *e1071* package (Meyer et al., 2014). The model also has the radial basis function (RBF) kernel, with two tuning parameters, *cost and gamma*. The former trades off misclassification of training of training examples against simplicity of the decision surface and the later sets the width of the kernel function (Cracknell and Reading, 2014). Both the classification building model and tuning were all performed using the *e1071* package (Meyer et al., 2014) and the *"best.tune"* function was used to build the SVM model by using equivalent functions in the e1071 package. Furthermore, a 10-fold cross-validation scheme in the *"best.tune"* function was used to derive the *"optimal"* parameter combinations, which were used for the classification model. The training data was divided into 10 subsets (k = 10), and the model was iteratively train on each of the 9 subsets (k-1) and validated on the remaining 1 subset during cross-validation process (Nyamekye et al., 2020).

2.3.3. Accuracy assessment for classification

This is essential in providing information about the classification performed (Abd El-Kawy et al., 2011). This is significant for individual image classification produced from any remote sensing image (Congalton and Green, 2019). It was tough to find reference data for LULC in the classification accuracy because of the long period between the images considered in this study. Points from Google Earth images and administrative maps were used as reference points for the accuracy assessment for each time periods. About 630 well distributed points were created for each LULC map, which was used for the accuracy assessment for each classified image. The points were divided into two;70% as training sample and 30% as test data. The F1-measure, overall accuracy (OA), and kappa coefficient were used for the accuracy assessment. The F1-measure which is used to assess the average class accuracy is the harmonic mean of user's accuracy and producer's accuracy (Daskalaki et al., 2006).

Table 1
Results from simulation showing the percentage of correctness and Kappa coefficient for validation of explanatory data with different criteria combination.

SN	Combination	Percentage of correctness	Kappa
1	Urban, slope, altitude	83.23	0.85
2	Road, population, slope	86.45	0.85
3	Altitude, Aspect, road, population, urban	84.84	0.79
4	Altitude, Aspect, road, population, urban, slope	83.12	0.81
5	Urban, road	81.89	0.78
6	Road, Altitude	82.10	0.83
7	Urban, Altitude	81.87	0.85

2.3.4. LULC modelling and prediction

The study adopted Clark Lab's Land Change Modeler (LCM) of TerrSet 18.21version software to predict LULC maps (2040 and 2060) using the classified LULC maps of 2010 and 2020. The LCM of TerrSet is used to analyse LULCC and empirical modelling as well as predicting future changes. The unified CA-Markov approach was adopted to run the future predictions (Islam et al., 2018). The 2010 and 2020 images were used to prepare the Transition Probability Matrix (TPM), Transition Probability Areas (TPA) and Transition Suitability Areas (TSA) from the Markov model. All these were combined into the CA-Markov model and the application of a 5*5 contiguity filter with 5 iterations to model (Nath et al., 2020) the LULC for the years 2040 and 2060.

2.3.5. Validation of CA-MARKOV model

The calibration and validation of the model is an essential phase for model prediction, because the accuracy of a model is based on the results of the model validation. The validation is performed by comparing the predicted and the actual LULC maps of 2020. This was achieved using the Kappa index of agreement and chi-square test (Nath et al., 2020), which is one of the common methods to quantify the predictive power of a model (Singh et al., 2017). Kappa coefficient is predominantly used in accuracy assessment of LULC (Rwanga and Ndambuki, 2017) to determine the right agreement between the observed and chance agreement (Sim and Wright, 2005). When the Kappa index is acceptable, the LULC map for 2040 and 2060 is predicted.

In this study, several criteria were used in the determination of the exploratory maps. A series of simulations were conducted to predict the LULC map of 2020 using a combination of criteria, for the exploratory data in simulating the LULC. The results of the analysis of the exploratory map from the simulations with combination of different variables is shown in Table 1. The results show that, percentage of correctness and Kappa coefficients are very high and close to each other. The exploratory data combination for road, population and slope produced the highest percentage of correctness and Kappa coefficient of 86.45% and 0.85 respectively. The highest Kappa values indicates that the three criteria being distance from road, population and slope (Fig. 3) have greater impact on the LULC change than the other criteria. Additionally, the transition matrices of the LULC classes between 2010 and 2020 is shown in Table 2. This was then used in the simulation to predict the map for the years 2040 and 2060.

3. Results

3.1. Temporal LULC changes over tropical rainforest

The classification maps were generated for the four years of study (Fig. 4). In 1986, the dominant LULC class was Open Forest with an area of 21,531.87 km^2. This was followed by Dense forest and Agricultural

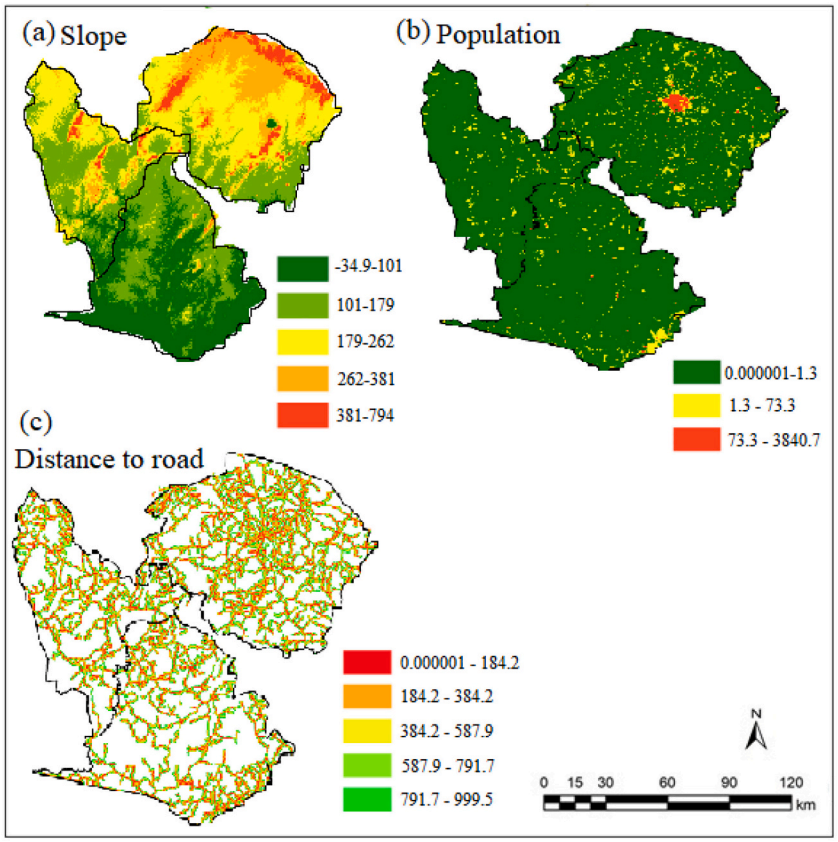

Fig. 3. Explanatory map for CA-MARKOV model; (a) slope (b) population and (c) distance from road.

land covering 21,531.89 km^2 and 1075.68 km^2, respectively. However, Mining recorded the smallest area of being 900.34 km^2 (Table 2). In 2002, Open Forest still constituted the largest LULC with an area of 20,284.45 km^2, with Agricultural land and Dense forest taking the second and third dominant class with an area of 1584.41 km^2 and 11,345.06 km^2, respectively. Additionally, Settlement and Mining increased to 5190.5 km^2 and 1208.29 km^2 respectively in the same year. Settlement and mining areas increased drastically to 9841.41 km^2 and 2555.70 km^2 in 2010, and 14,518.82 km^2 and 9071.58 km^2 in 2020 respectively. On the contrary, Open and Dense Forest decreased immensely by 3.02% and 1.52%, respectively between 2010 and 2020. The trend of settlement and mining increased throughout the period of study (1986 to 2020) by 26.69 and 30.31% per annum, respectively. On the contrary, Open and Dense Forest have undergone reduction of 1.25% and 1.50% area coverage, respectively from 1986 to 2020. Thus, Open Forest reduced from 21,531.87 km^2 to 14,518.82 km^2 and Dense Forest reduced from 14,313 km^2 to 8202.98 km^2 over a period of 34 years. Water also experienced an annual reduction of 1.92% from 1986 to 2020. Additionally, the gains/losses and rates of change of LULC for each class was determined for each period and presented in Table 2. The period (2010−2020) experienced much increase and decrease in the rate of change with values of 32.09 and 7.41% per annum respectively. This was followed by 1986–2020 with an annual positive and negative rate of change of 24.09 and 4.04%, respectively (Table 3). However, 2002–2010 experienced relatively less change with a positive and negative rate of change of 13.09 and 3.83%, respectively The Overall Accuracies (OA) of the LULC classification for the four years (1986, 2002, 2010 and 2020) were 93.27, 90.57, 91.61 and 93.23%, respectively (Table 4). The Kappa statistics of the classified images were 0.90, 0.87, 0.86, 0.93 for 1986, 2002, 2010 and 2020 respectively, these values were above 0.80 (80%) showing a strong level of agreement of classification accuracy (Congalton and Green, 2019; Odame Appiah, 2016). The results showed an OA and Kappa statistics greater than 90% and 0.85, which is higher than the accepted OA threshold of 85% for LULC classifications (Anderson et al., 1976). Additionally, the F1 score, which is the harmonic mean for user's and producer's accuracy were found to be more than 80% for all the classified satellite images (Table 3).

3.2. Spatial trend of LULC

Figs. 5 and 6 show the change in spatial trend of LULC and also provides the intensity of change along with the direction. This is very essential in identifying the critical zone where massive changes occurred in the period considered in the study. The main purpose of the spatial trend map is to show the general overview of the pattern of variations of change in the land use class. Vegetation (Dense and Open forest) are deemed as the most important land use in this research. Hence, the trend of change from these classes compared with other land use are displayed in the spatial trend map. For example, the spatial trend from Dense Forest to mining and settlement for 2010–2020 period are shown in Fig. 5, while Fig. 6 show the change from Open forest to Mining and settlement for 2010–2020. The value of change was significant after applying five polynomial order, a positive value represents change from

Table 2
Area, magnitude and rates of LULC changes of the study area.

LULC Class	Area/km^2				Gain/loss between different time periods/km^2				Rate per annum (%)			
	1986	2002	2010	2020	1986–2002	2002–2010	2010–2020	1986–2020	1986–2002	2002–2010	2010–2020	1986–2020
Agricultural land	1075.68	1584.41	1744.51	2068.84	508.73	160.09	324.33	993.15	2.95	0.63	1.85	2.71
Dense forest	14,313.15	11,345.06	9673.44	8202.98	−2968.08	−1671.62	−1470.46	−6110.1	−1.29	−0.92	−1.52	−1.25
Mining	900.34	1208.29	2555.70	9071.58	307.95	1347.40	6515.87	8171.23	2.13	6.96	25.49	26.69
Open forest	21,531.87	20,284.45	15,069.22	10,507.75	−1247.41	−5215.23	−4561.46	−11,024.11	−0.36	−1.60	−3.02	−1.50
Settlement	1283.89	5190.51	9841.42	14,518.82	3906.62	4650.90	4677.40	13,234.93	19.01	5.60	4.75	30.31
Water	1324.90	817.09	645.50	459.95	−507.80	−171.58	−185.55	−864.94	−2.39	−1.31	−2.87	−1.92

the category in focus to others, while the negative value represents the gain. The dark red colour indicates the severity of change. For example, Fig. 5b shows a darker red colour than Fig. 5a when the spatial coverage of change is considered. This is an indication that the changes that occurred from Dense forest to settlement was more intense than the change that occurred from Dense to Mining., It was observed that, the change in the south-eastern part was intense than the other areas of the study, though the change started from the northern part of the area (Fig. 5a). In view of this, it could be mentioned that the south-eastern part of the study is highly vulnerable to change from Dense forest to Mining. Additionally, it can be seen from Fig. 5b that, the north-eastern part of the study is highly vulnerable to change from Dense forest to settlement. Furthermore, the north-western part of the study, as shown in Fig. 6a, is highly vulnerable to conversion from Open forest to Mining, while in Fig. 6b, the north-eastern part of the study is rather extremely sensitive to change from open forest to settlement.

3.3. Validation of predicted LULC

The actual land use of 2020 was compared with the simulated land use of 2020 (Fig. 7).

The results of the chi-square test for the model validation are shown in Table 4 and Fig. 8. The null hypothesis was that, there was no significant change in the area statistics of the actual and the simulated land use of 2020. Nonetheless, the spatial distribution of different land use categories was not validated by the test. The null hypothesis was accepted because the value of the observed chi-square was greater than that of the calculated chi-square (Table 5), which makes the model suitable to predict the Land Use Land Cover for the future years.

Also, the chi-square test does not essentially validate the agreement on the spatial distribution of the LULC classes. In order to overcome this problem, quantity agreement and allocation disagreement was also adopted for the validation of the model. The results of the model validation show that overall agreement between actual and simulated maps of 2020 is 0.942, while overall simulation error is 0.018. The simulation error can be further partitioned into 0.015 (error due to quantity/ Disagreement Quantity) and 0. 035 (error due to allocation/disagreement grid cell). Thus, the validation shows that the major disagreement between the two maps was due to an allocation error, with the disagreement quantity between the actual and simulated land use of 2020 showing a good predicting ability (Table 5).

Additionally, the Kappa indices (k-indices) were also used to test the accuracy of the simulation. These values for the indices are 0.89, 0.91 and 0.86 for K-no, Klocation and Kstandard respectively (Table 6). The value for the ROC for the simulation is 0.9, which is the correlation between the simulated and actual land use changes (Pontius and Millones, 2011). All the results of the index agreement depicted an average value of 0.89, which indicates that the simulation can considerably be used to accurately predict both the quantity and location of change. According to (Zadbagher et al., 2018), a model is valid when the overall Kappa (Kstandard) exceeds 0.7 (70%).

3.4. Land use land cover projection

The CA-MARKOV model used is a good fit for predicting the future land use change of the study area. Thus, the predicted LULC for the different time periods 2040 and 2060 was produced (Fig. 9 a and b), based on the successful simulation of LULC changes in 2020 (Fig. 7). The descriptive statistics (Table 7) showed that from 2020 to 2040, the study area would experience a higher change in Settlement (1.40%) per annum between 2040 and 2060 than the two other time periods, suggesting a swift conversion of other LULC to settlement in study area. Open forest would also experience annual decrease of 1.33% from 2020 to 2040, which is higher than the decrease experienced in the other time periods. Furthermore, the Dense forest would experience a negative change of 0.21% between 2020 and 2040, which is higher when

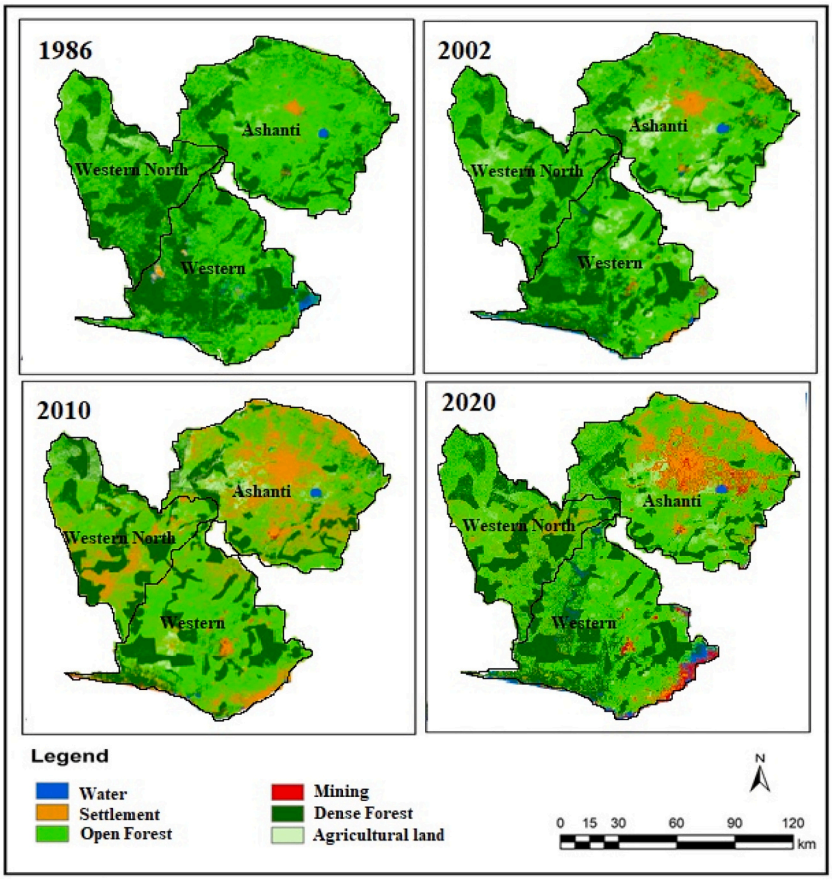

Fig. 4. The classified maps of 1986, 2002, 2010 and 2020.

Table 3
Accuracy assessment results showing F 1 score, Overall accuracy and Kappa coefficient.

Classification accuracy	1986	2002	2010	2020
F 1 score %	83.44	88.56	84.35	89.13
Overall Accuracy %	93.27	90.57	91.61	93.23
Kappa coefficient	0.90	0.87	0.86	0.95

Table 4
Validation of the predicted LULC based on the simulated and actual 2020 LULC change.

Chi-Square test			
LULC Classes	Simulated LULC in 2020 (O)	Actual LULC in 2020 (E)	$(O-E)^2/E$
Agricultural land	12.76	16.32	0.78
Dense forest	35.23	39.69	0.50
Mining	12.76	6.87	5.05
Open forest	11.35	14.26	0.59
Settlement	8.67	8.21	0.03
Water	19.23	14.65	1.43
Total	100	100	8.37

$\chi^2 = \sum \frac{(O-E)2}{E} = 8.37$; df = 5 and: $\chi^2_{0.05}(5) = 8.40$.

compared with the negative change in the other two time periods. It is an indication that the areas of Open and Dense forest will be at risk in the future due to its faster rate of depletion. Additionally, the percentages of Agricultural land and water were projected to decrease by approximately 0.40% and 0.75% from 2020 to 2040 and 0.48% and 0.25% from 2040 to 2060 respectively. However, Mining is projected to increase by 1.81% from 2020 to 2040, and decrease by 4.56% from 2040 to 2060. Settlement is projected to increase by 3.45% and 2.87% from 2020 to 2040 and 2040 to 2060 respectively. The differences between the 2020 LULC map and 2060 show the massive increase in settlement by 3.07%.

4. Discussion

4.1. Dynamics of LULC and major drivers of change

The spatio-temporal aspects of LULC changes between 1986 and 2020 have been analyzed for the study using remotely sensed data and field validation. The study shows that land degradation and forest depletion are extensive in the area of study. The increase of illegal mining, firewood cutting, charcoal production and clearing of land for farming threatens the existing vegetation cover. These drivers might be the greatest contributors to forest degradation in the forested areas. The significant decrease in vegetation cover (Dense and Open Forest) from 35,845.02 km^2 to 18,710.73 km^2 observed between 1986 and 2020 could be associated to increase in poverty and population increase. Additionally, this decrease in vegetation could be as a result of increase in illegal mining, indiscriminate firewood cutting, inefficient charcoal

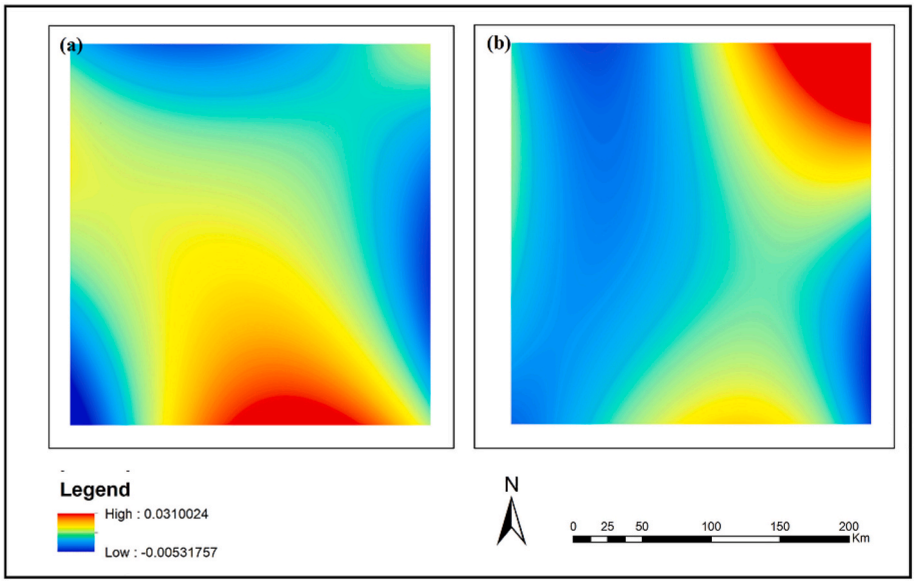

Fig. 5. Spatial trend of land use from (a) Dense forest to Mining (b) Dense forest to settlement.

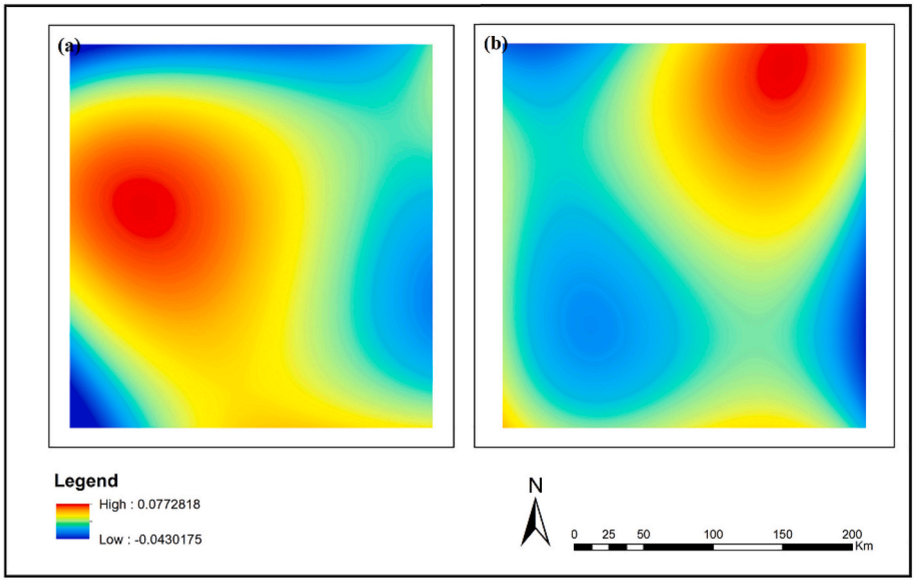

Fig. 6. Spatial trend of land use from (a) Open forest to Mining (b) Open forest to settlement.

production methods and clearing of land for crop farming. The LULC change model for this study used an empirical statistic of the past to project the future changes, the outcome represents the LULC changes in the business-as-usual scenario. Thus, the results from this projection help to understand and depict how essential drivers of change will affect the land cover changes, if left unregulated. Additionally, agricultural expansion, wood extraction for timber, construction material and fire-wood are some of the drivers of LULC change in the study area. Also, the increase in urban population resulting in demand for food and shelter causes expansion in agriculture and settlement areas, thereby affecting the LULC changes. Thus, in the absence of reformed regulatory measures, legal policies and frameworks, the study area will continue to be threatened by illegal mining, encroachment and deforestation, which are primarily caused by rural- urban migration and poverty.

The demographic data from (Ghana Statistical Service, 1984 2000 and Ghana Statistical Service, 2010) were used to assess the trends of population change over the period of study and compare with the LULC change. The report from the GSS for 2000 and 2010 showed that the population of the study area have increased from 5,537,527 in 2000 to 7,156,401 in 2010, while urban population of increased from 43.8% to 51.5% respectively (GSS, 2010). The driver (population) has been mentioned as the cause of LULC change in the study, which corroborates with results from other studies (e.g., Hassen and Assen, 2018; Minta et al., 2018). Similarly, Denboba (2005) also reported that forest depletion is mostly caused by the expansion of settlements and agricultural lands due to population increase and socioeconomic changes. Other studies also reported that, growth in population, increase in settlement areas and agricultural lands are among the major drivers of

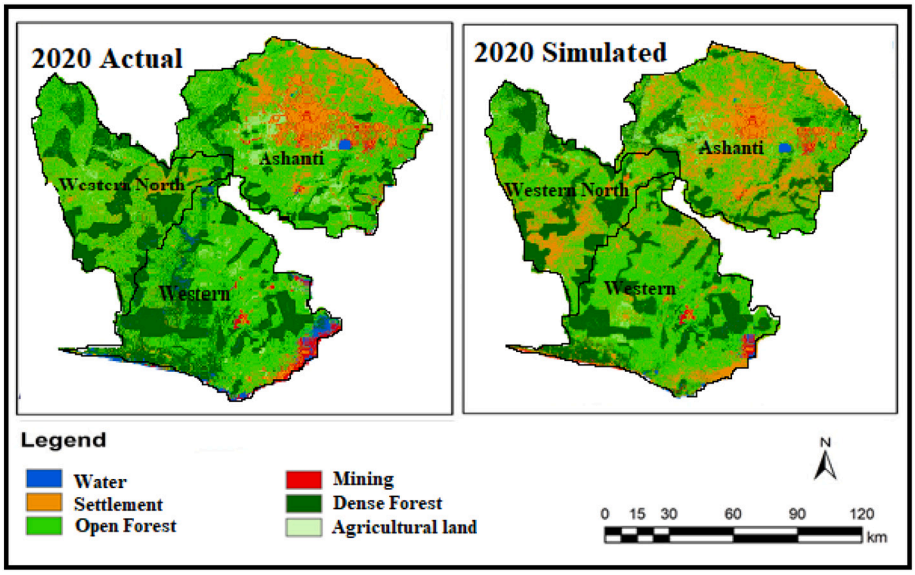

Fig. 7. Actual and simulated LULC map of study area (tropical rainforest) using ANN model.

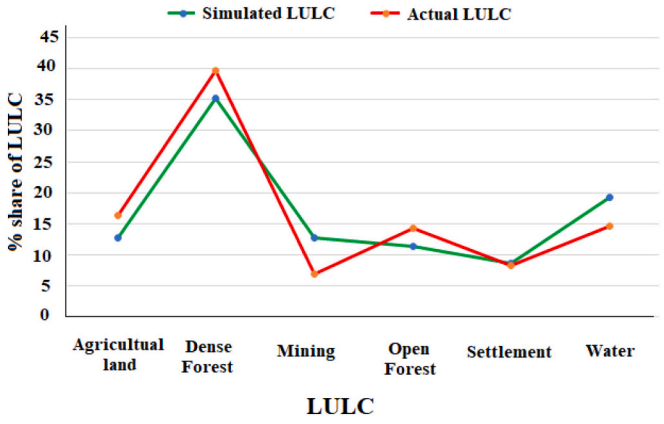

Fig. 8. Areas of simulated against actual LULC classes in the year 2020 in percentage.

Table 5
Validation analysis of two images.

Agreement/Disagreement	Value %
Agreement chance	18
Agreement quantity	56.78
Agreement grid-cell	20.23
Disagreement grid-cell	3.52
Disagreement quantity	1.51

Table 6
Accuracy assessment of the simulated land use image of 2020.

Index	Value
Kno	0.89
Klocation	0.91
ROC	0.90
Kstandard	0.86

LULC change in Ethiopia (Kindu et al., 2015; Gebrelibanos and Assen, 2015; Yesuf et al., 2015).

4.2. The LULC change impact on the tropical rainforest of Ghana

The degradation of the land starts with the loss of vegetation cover. One of the major factors that determines the rate of degradation in vegetation cover is LULC change (Gebrelibanos and Assen, 2015). The removal of the vegetation cover results in soil erosion, which increase the creation of sheet, rill and gully erosions due to the reduction in soil cover. Also, the removal of the forest cover through illegal practices could influence the hydrological processes and, eventually increase the rate of soil erosion (Dagnachew et al., 2020). Considering the observed LULC changes in the Dense forest and Open forest, the tropical rainforest could be prone to soil erosion. In view of this, 88.66%, 78.23%, 61.19%, and 57.56% of total area of study site in 1986, 2002, 2010 and 2020 respectively were potentially exposed to soil erosion (Table 2). Therefore, the expansion of agricultural land and mining areas could increase the susceptibility of soil to erosion. Thus, the loss of forest (Dense and Open) cover at the expense of agriculture, mining and settlement could have an immense implication on soil erosion, which in turn causes sedimentation in the river bodies. Additionally, the large-scale deforestation and conversion to agriculture and mining would immensely affect the landscape and cause adverse effects on biodiversity, soil degradation and also undermines the natural resources, on which the local population depend.

It is therefore paramount, to form adequate spatial policies to balance the competing needs for land to augment the accelerating population and provide resources, while minimizing the loss of biodiversity and ecosystem. The Sustainable Development Goals (SDGs) offer the blueprint for such policy planning and interventions, focusing on balancing prosperity for both earth and the people. The expansion of agricultural land and direct exploitation of the natural resource through mining activities is linked with the economic condition of the populace. Thus, the policies should focus on improving and strengthening the economic security and livelihood of the people in the study area, in order to protect the biodiversity and ecosystem in the study area.

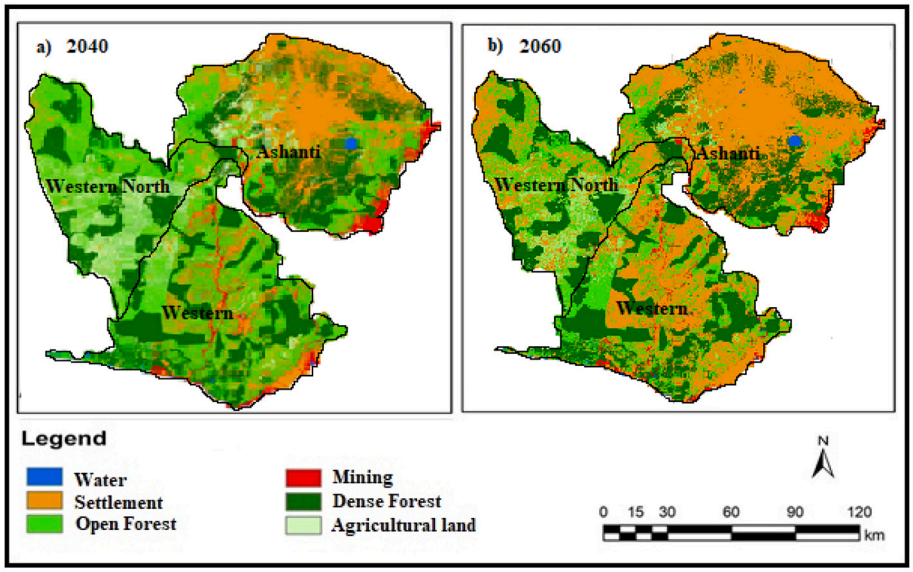

Fig. 9. a) Predicted LULC map of 2040 b) Predicted LULC map of 2060.

Table 7
Predicted area statistics of LULC for 2040 and 2060.

LULC class	Area/km^2			Predicted gain/loss between different time periods/km^2			Rate per annum (%)		
	2020	2040	2060	2020–2040	2040–2060	2020–2060	2020–2040	2040–2060	2020–2060
Agricultural land	2068.84	1899.22	1667.78	−169.61	−231.44	−401.05	−0.40	−0.60	−0.48
Dense forest	8202.98	7844.4	7594.4	−358.58	−250	−608.58	−0.21	−0.15	−0.18
Mining	9071.58	12,371.04	1081.04	3299.46	−11,289.99	−7990.53	1.81	−4.56	−2.20
Open forest	10,507.75	7707.39	5807.39	−2800.36	−1900	−4700.36	−1.33	−1.23	−1.11
Settlement	14,518.82	18,602.63	20,802.63	4083.80	2200	6283.80	1.40	0.59	1.08
Water	459.95	390.24	412.24	−69.71	21.99	−47.71	−0.75	0.28	−0.25

5. Conclusion

This study shows the trend of LULC change from 1986 to 2020. It was observed that the tropical rainforest has undergone massive degradation within the period of study (1986–2020). Intense pressure due to unregulated anthropogenic activities such as illegal mining are causing the area to rapidly loose its environmental and biotic integrity. About, 35,845.02 km^2 of the total land mass was covered by forest in 1986 representing 88.65% of the total land. However, the study showed that rapid change of the forest cover to other LULC has reduced to 18,710.73 km^2 in 2020. This phenomenon indicates that the study area has lost almost 47% of its vegetation cover over the 34-year period. The trend of LULC change shows that vegetation cover is on the decline, whereas settlement and mining is on the rise. Consequently, the vegetation cover available for the CO_2 sequestration is declining, thereby rapidly increasing the country's carbon footprint in the long term.

Additionally, the application of CA- Markov model for the prediction of future land use show that the model is a good fit to describe the LULC of the area for 2040 and 2060. The results from the simulation indicate that forest cover will be about 18,710.73 km^2 in 2020 and 15,551.79 km^2 and 13,401.79 km^2 in 2040 and 2060 respectively. The overall accuracy of prediction using CA-Markov model is above 80%, which is very satisfactory. The incorporation of the driver variables (slope, population and distance to road) identified the potential factors for LULC conversion in the study site. The drivers and dynamics of LULC changes is important in developing sustainable land management policies and socio-economic reforms in the quest to initiate conservation actions and management practices to protect biodiversity and ecosystem services of the study area.

Declaration of Competing Interest

The authors declare no competing of interest.

Acknowledgements

The authors are grateful to Koforidua Technical University for their support. We acknowledge the USGS-NASA for their freely accessible Landsat images. Finally, we also appreciate comments from all those who reviewed the manuscript to improve the quality.

References

Abd El-Kawy, O.R., Rød, J.K., Ismail, H.A., Suliman, A.S., 2011. Land use and land cover change detection in the western Nile delta of Egypt using remote sensing data. Appl. Geogr. 31, 483–494.

Acheampong, M., Yu, Q., Enomah, L.D., Anchang, J., Eduful, M., 2018. Land use/cover change in Ghana's oil city: assessing the impact of neoliberal economic policies and implications for sustainable fevelopment goal number one – A remote sensing and GIS approach. Land Use Policy 73, 373–384. https://doi.org/10.1016/j.landusepol.2018.02.019.

Ahmed, B., Ahmed, R., 2012. Modeling urban land cover growth dynamics using multitemporal satellite images: a case study of Dhaka, Bangladesh. ISPRS Int. J. Geo-Inf. 1, 3–31. https://doi.org/10.3390/ijgi1010003.

Anderson, J.R., Hardy, E.E., Roach, J.T., Witmer, R.E., 1976. A Land Use and Land Cover Classification System for Use with Remote Sensor Data. Government Printing Office, Washington, DC, USA, 573, p. 325.

Asabere, S.B., Acheampong, R.A., Ashiagbor, G., Beckers, S.C., Keck, M., Erasmi, S., Schanze, J., Sauer, D., 2020. Urbanization, land use transformation and spatio-environmental impacts: analyses of trends and implications in major metropolitan regions of Ghana. Land Use Policy 96, 104707. https://doi.org/10.1016/j.landusepol.2020.104707.

Beaumont, L.J., Duursma, D., 2012. Global projections of 21st century land-use changes in regions adjacent to protected areas. PLoS One 7 (8), 1–8. https://doi.org/10.1371/journal.pone.0043714.

Congalton, R.G., Green, K., 2019. Assessing the Accuracy of Remotely Sensed Data: Principles and Practices. CRC press.
Cracknell, M.J., Reading, A.M., 2014. Geological mapping using remote sensing data: a comparison of five machine learning algorithms, their response to variations in the spatial distribution of training data and the use of explicit spatial information. Comput. Geosci. 63, 22–33.
Dagnachew, M., Kebede, A., Moges, A., Abebe, A., 2020. Land use land cover changes and its drivers in Gojeb River catchment, Omo Gibe Basin, Ethiopia. J. Agric. Environ. Int. Dev. 114, 33–56.
Daskalaki, S., Kopanas, I., Avouris, N., 2006. Evaluation of classifiers for an uneven class distribution problem. Appl. Artif. Intell. 20, 381–417.
Denboba, M.A., 2005. Forest coversion - soil degradation - Farmers´ perception nexus: implications for sustainable land use in the southwest of Ethiopia. Ecol. Dev. Ser. 26 (49). https://cuvillier.de/de/shop/publications/2579.
Devlelopment Core Team, R, 2013. R: A Language and Environment for Statistical Computing.
Gebrelibanos, Tsehaye, Assen, Mohammed, 2015. Land use/land cover dynamics and their driving forces in the Hirmi watershed and its adjacent agro-ecosystem, highlands of northern Ethiopia. J. Land Use Sci. 10 (1), 81–94.
Ghana Statistical Service, 2010. Population and housing census - Summary report of final results. In: Ghana Statistical Service. http://www.statsghana.gov.gh/docfiles/2010phc/Census2010_Summary_report_of_final_results.pdf.
Hamad, R., Balzter, H., Kolo, K., 2018. Predicting land use/land cover changes using a CA- Markov model under two different scenarios. Sust. 10, 3421.
Haque, M.I., Basak, R., 2017. Land cover change detection using GIS and remote sensing techniques: a spatio-temporal study on Tanguar Haor, Sunamganj, Bangladesh. Egypt J. Remote Sens. Sp. Sci. 20, 251–263. https://doi.org/10.1016/j.ejrs.2016.12.003.
Hassen, E.E., Assen, M., 2018. Land use/cover dynamics and its drivers in Gelda catchment, Lake Tana watershed, Ethiopia. Environ. Syst. Res. 6 (1), 1–13. https://doi.org/10.1186/s40068-017-0081-x.
Herold, M., Scepan, J., Clarke, K., 2002. The use of remote sensing and landscape Metrices to describe structures and changes in urban land uses. Environ. Plan. A 34 (8), 1443–1458. https://doi.org/10.1068/a3496.
Islam, K., Jashimuddin, M., Nath, B., Nath, T.K., 2018. Land use classification and change detection by using multi-temporal remotely sensed imagery: the case of Chunati wildlife sanctuary, Bangladesh. Egypt J. Remote Sens. Sp. Sci. 21, 37–47. https://doi.org/10.1016/j.ejrs.2016.12.005.
Kindu, Mengistie, Schneider, Thomas, Teketay, Demel, Knoke, Thomas, 2015. Drivers of land use/land cover changes in Munessa-Shashemene landscape of the south-central highlands of Ethiopia. Environ. Monit. Assess. 187 (7).
Kogo, B.K., Kumar, L., Koech, R., 2019. Analysis of spatio-temporal dynamics of land use and cover changes in Western Kenya. Geocarto Int. 36, 376–391.
Kutiote, E.K., Tarlue, P.J., Umar, N.A., Chanda, P., Aisha-Lul, A.N., Nalumansi, P., Nina, P.M., 2019. Deforestation of Igwe Forest and its effects on livelihood patterns of peripheral communities in Bugiri District, Uganda. African J. Agric. Food Sci. 2, 41–53.
Langat, P.K., Kumar, L., Koech, R., Ghosh, M.K., 2019. Monitoring of land use/land-cover dynamics using remote sensing: a case of Tana River Basin, Kenya. Geocarto Int. 1–19.
Liu, S., Wang, X., Liu, M., Zhu, J., 2017. Towards better analysis of machine learning models: a visual analytics perspective. Vis. Informatics 1, 48–56.
Lossou, E., Owusu-Prempeh, N., Agyemang, G., 2019. Monitoring land cover changes in the tropical high forests using multi-temporal remote sensing and spatial analysis techniques. Remote Sens. Applic. Soc. Environ. 16, 100264 https://doi.org/10.1016/j.rsase.2019.100264.
Meyer, D., Dimitriadou, E., Hornik, K., Weingessel, A., Leisch, F., 2014. e1071: Misc Functions of the Department of Statistics (e1071). TU Wien. R package version 1.6-3.
Minta, M., Kibret, K., Thorne, P., Nigussie, T., Nigatu, L., 2018. Land use and land cover dynamics in Dendi-Jeldu hilly-mountainous areas in the central Ethiopian highlands. Geoderma 314, 27–36. https://doi.org/10.1016/j.geoderma.2017.10.035.
Mountrakis, G., Im, J., Ogole, C., 2011. Support vector machines in remote sensing: a review. ISPRS J. Photogramm. Remote Sens. 66, 247–259.
Muriithi, F.K., 2016. Land use and land cover (LULC) changes in semi-arid sub-watersheds of Laikipia and Athi River basins, Kenya, as influenced by expanding intensive commercial horticulture. Remote Sens. Appl. Soc. Environ. 3, 73–88.
Näschen, K., Diekkrüger, B., Evers, M., Höllermann, B., Steinbach, S., Thonfeld, F., 2019. The impact of land use/land cover change (LULCC) on water resources in a tropical catchment in Tanzania uder Dirrerent climate change scenarios. Sust. 11, 1–28. https://doi.org/10.3390/su11247083.
Nath, B., Wang, Z., Ge, Y., Islam, K.P., Singh, R., Niu, Z., 2020. Land use and land cover change modeling and future potential landscape risk assessment using Markov-Ca model and analytical hierarchy process. ISPRS Int. J. Geo-Information 9, 134.
Nyamekye, C., Kwofie, S., Ghansah, B., Agyapong, E., Boamah, L.A., 2020. Assessing urban growth in Ghana using machine learning and intensity analysis: a cased study of the new Juaben Municipality. Land Use Policy 99, 105057.
Odame Appiah, D., 2016. Geoinformation Modelling of Peri-Urban Land Use and Land Cover Dynamics for Climate Variability and Climate Change in the Bosomtwe District, Ghana. PhD Thesis. KNUST.
Oduro, K.A., Mohren, G.M.J., Peña-Claros, M., Kyereh, B., Arts, B., 2015. Tracing forest resource development in Ghana through forest transition pathways. Land Use Policy 48, 63–72. https://doi.org/10.1016/j.landusepol.2015.05.020.
Pontius, R.G., Millones, M., 2011. Death to kappa: birth of quantity disagreement and allocation disagreement for accuracy assessment. Int. J. Remote Sens. 32 (15), 4407–4429. https://doi.org/10.1080/01431161.2011.552923.
Rwanga, S.S., Ndambuki, J.M., 2017. Accuracy assessment of land use/land cover classification using remote sensing and GIS. Int. J. Geosci. 8, 611.
Satyal, P., 2018. Civil society participation in REDD+ and FLEGT processes: case study analysis from Cameroon, Ghana, Liberia and the Republic of Congo. For. Policy Econ. 97, 83–96. https://doi.org/10.1016/j.forpol.2018.09.012.
Sim, J., Wright, C.C., 2005. The kappa statistic in reliability studies: use, interpretation, and sample size requirements. Phys. Ther. 85, 257–268.
Simms, D., 2008. The effects of urbanization on natural resources. In: 44th ISOCARP Congress 2008, pp. 1–12.
Singh, S.K., Laari, P.B., Mustak, S.K., Srivastava, P.K., Szabó, S., 2017. Modelling of land use land cover change using earth observation data-sets of Tons River Basin, Madhya Pradesh, India. Geocarto Int. 33, 1202–1222.
Sinha, S., Sharma, L.K., Nathawat, M.S., 2015. Improved land use/land cover classification of semi-arid deciduous forest landscape using thermal remote sensing. Egypt. J. Rem. Sens. Sp. Sci. 18 (2), 217–233. https://doi.org/10.1016/j.ejrs.2015.09.005.
Sivakumar, V., 2014. Urban mapping and growth prediction using remote sensing and GIS techniques, Pune, India. ISPRS – Int. Arch. Photogram. Rem. Sens. Spa. Inf. Sci. XL-8, 967–970.
Subedi, P., Subedi, K., Thapa, B., 2013. Application of a hybrid cellular automaton–Markov (CA–Markov) model in land-use change prediction: a case study of saddle creek Drainage Basin, Florida. Appl. Ecol. Environ. Sci. 1, 126–132. https://doi.org/10.12691/aees-1-6-5.
Trisurat, Y., Shirakawa, H., Johnston, J.M., 2019. Land-use/land-cover change from socio-economic drivers and their impact on biodiversity in Nan Province, Thailand. Sustain. 11 https://doi.org/10.3390/su11030649.
Vapnik, V., 2013. The Nature of Statistical Learning Theory. Springer science & business media.
Yang, Y., Bao, W., Li, Y., Wang, Y., Chen, Z., 2020. Land use transition and its eco-environmental effects in the Beijing-Tianjin-Hebei urban agglomeration: a production-living-ecological perspective. Land 9. https://doi.org/10.3390/LAND9090285.
Yesuf, Hassen M., Assen, Mohammed, Alamirew, Tena, Melesse, Assefa M., 2015. Modeling of sediment yield in Maybar gauged watershed using SWAT, Northeast Ethiopia. Cat. 127, 191–205.
Zadbagher, E., Becek, K., Berberoglu, S., 2018. Modeling land use/land cover change using remote sensing and geographic information systems: case study of the Seyhan Basin, Turkey. Environ. Monit. Assess. 190 (8) https://doi.org/10.1007/s10661-018-6877-y.
Zeng, Q., Gu, W., Zhang, X., Wen, H., Lee, J., Hao, W., 2019. Analyzing freeway crash severity using a Bayesian spatial generalized ordered logit model with conditional autoregressive priors. Accid. Anal. Prev. 127, 87–95. https://doi.org/10.1016/j.aap.2019.02.029.